



Full length article

Dynamic deformation and failure of ultrafine-grained titanium



Ze Zhou Li^a, Bingfeng Wang^b, Shiteng Zhao^a, Ruslan Z. Valiev^c, Kenneth S. Vecchio^a, Marc A. Meyers^{a,*}

^a University of California, San Diego, La Jolla, CA 92093, USA

^b Central South University, Changsha 410083, PR China

^c Institute of Physics of Advanced Materials, Ufa State Aviation Technical University, Ufa 450000, Russia

ARTICLE INFO

Article history:

Received 27 August 2016

Received in revised form

16 November 2016

Accepted 17 November 2016

Keywords:

Ultrafine-grained titanium

Constitutive response

Adiabatic shear band formation and failure mechanism

ABSTRACT

Dynamic deformation and shear localization of ultrafine-grained (~120 nm) pure titanium are examined. The strain hardening can be considered as having two regimes: below and above a strain ~0.04; at this point there is a drastic decrease in the slope. The strain-rate sensitivity of ultrafine-grained titanium is found to be approximately the same as its coarse grained counterpart. Based on experimentally determined parameters, the Zerilli-Armstrong equation is modified to describe the mechanical response of the ultrafine-grained titanium over the strain rate range 10^{-5} to 10^3 s⁻¹. Adiabatic shear banding is examined in a forced shear configuration where large strain is imposed in a narrow region. The microstructure inside the adiabatic shear band consists of a mixture of elongated grains and equiaxed nanograins (~40 nm) that are significantly smaller than the initial grains (~120 nm). The formation of equiaxed nanograins is modeled through a mechanism of rotational dynamic recrystallization. This further reduction in grain size from the one generated by ECAP is interpreted in terms of the Zener-Hollomon parameter for quasistatic and dynamic deformation. The adiabatic shear band eventually fractures by a combination of brittle and ductile failure.

© 2016 Acta Materialia Inc. Published by Elsevier Ltd. All rights reserved.

1. Introduction

Ultrafine-grained (UFG) and nanocrystalline metals have been the subject of widespread research over the past couple of decades with significant acceleration in recent years [1]. As the name suggests, nanocrystalline materials are single or multi-phase polycrystals with nano-scale (1–100 nm) grain size. At the upper limit of this regime, the term “ultrafine grain size (UFG)” is often used (grain sizes of 100–1000 nm) [2]. Most studies on the failure behavior of UFG and nanocrystalline materials have mainly focused on the phenomena occurring under static or quasi-static loading, whereas research on dynamic properties under high strain rates is rare. Shear bands are often sites of initiation and growth for subsequent dynamic fracture [3,4].

There have been a number of investigations on the dynamic behavior of α -titanium with different grain sizes. Meyers et al. [5] investigated dynamic response and shear-band formation of CP grade 2 titanium with a grain size ~72 μ m in high strain-rate plastic

deformation. Micrograins smaller than the initial grain size were observed within the shear band and attributed to the dynamic recovery/recrystallization. Ko et al. [6] and Liu et al. [7] studied mechanical behavior of UFG pure titanium (~300 nm) and showed that it exhibited a significant improvement in yield strength with an absence of strain hardening behavior compared with coarse grained titanium. However, dynamic behavior of UFG titanium with grain size significantly below 300 nm, especially shear localization, still remains largely unexamined.

2. Experimental procedure

The as-received UFG pure titanium samples investigated were 200 mm long and 6 mm diameter rods processed by ECAP-C technique, according to a general procedure presented elsewhere [8,9]. The average grain size of the as-received UFG titanium was ~120 nm. The microstructure of cross-section of as-received titanium rod was observed by Lopes et al. [10] using transmission electron microscope (TEM) as shown in Fig. 1. Dynamic compression tests were performed using a split Hopkinson pressure bar (SHPB). Dynamic response and shear deformation were measured using cylindrical and hat-shaped specimens. The cylinders had a

* Corresponding author.

E-mail address: mameyers@eng.ucsd.edu (M.A. Meyers).

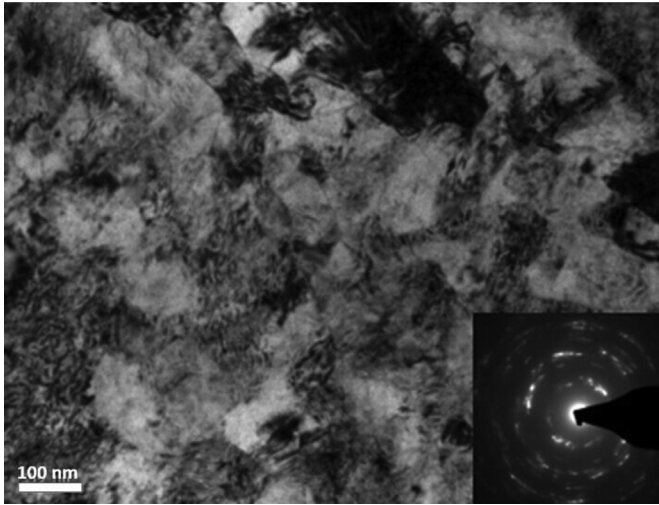


Fig. 1. TEM image of the as-received titanium rod [10].

length and diameter of 4 mm. Hat-shaped specimens were used to generate high shear strain in the “forced” localized region [11]. Fig. 2(a) illustrates their geometry and dimensions. The details and principles of this procedure are discussed by Meyers et al. [11] and have been used for the formation of adiabatic shear bands in coarse grained titanium [12].

The deformed hat-shaped samples were cut parallel to the shear band for microstructural examination. A diamond saw at a speed of 600 rpm and a feed speed of approximately 0.01 mm/s was used. The etching solution for UFG titanium was 2.5 ml HF, 3 ml HNO₃, 5 ml HCl and 91 ml H₂O. The shear band was examined in a Phillips XL30 scanning electron microscopy (SEM). A focused ion beam (FIB) instrument was used to accurately prepare TEM samples in the shear band regions. The FIB specimen orientation is shown in Fig. 2(b). Figs. 2(c) and (d) further show the FIB sections in samples B and C, which are perpendicular to shear band and along shear band, respectively. The specimens were characterized by TEM using a FEI Tecnai G² Polara transmission electron microscope operating at 200 kV.

3. Results and discussion

3.1. Mechanical properties of UFG titanium

3.1.1. Strain hardening and strain-rate sensitivity

Fig. 3(a) shows the room-temperature compression stress-

strain curves at different strain rates. After an initial stage of rapid strain hardening, the strain-hardening rate beyond a strain of 0.04 is significantly reduced. This is characteristic of nanocrystalline and UFG materials, which often show low strain-hardening rate. Fig. 3(b) further shows that the strain-hardening rate of UFG titanium under dynamic loading follows the same trend. In contrast, the flow stress of coarse-grained polycrystalline titanium under dynamic loading continues to increase [5]. The density of dislocations in a nanocrystalline metal saturates due to dislocation annihilation at grain boundaries. UFG Ti thus loses its defect accumulation ability and hence the capacity for strain hardening. However, dislocations are still the carriers of plastic deformation until the grain size is in the range of 10–15 nm. Flat compression curves have been observed for UFG pure titanium made by ECAP [13]. Elias et al. [14] also reported a low strain-hardening rate for UFG titanium having a grain size ~200 nm after a strain of 0.05.

The strain-rate dependence of the yield stress for two grain sizes (72 μm and 120 nm) is shown in Fig. 3(c). The strain-rate sensitivity, defined as $m = \partial \log \sigma / \partial \log \dot{\epsilon}$, is 0.027 between 10^{-4} s^{-1} and 10^3 s^{-1} for both UFG titanium and coarse-grained titanium [5,15]. At the higher strain-rate, there is an increase in m . The activation volume parameter concept provides insight into the deformation mechanisms [16]. It is expressed as:

$$v^* = \frac{kT}{m\sigma_y} \quad (1)$$

where T is the temperature, σ_y is the yield stress, and k is Boltzmann constant. It can be seen from Eqn. (1) that the activation volume v^* is inversely proportional to both the strain-rate sensitivity and yield stress. The yield stress of UFG titanium is approximately twice that of coarse-grained CP titanium. The activation volume of UFG pure titanium is $\sim 6b^3$, where $b = 0.289 \text{ nm}$ is the Burgers vector in hexagonal titanium. This represents a significant reduction in the activation volume, compared with $80b^3$ for coarse-grained CP titanium [10], suggesting a change in the rate controlling mechanism. The influence of the cutting of forest dislocations decreases for UFG materials. This results in a decrease of the activation volume related to its low strain-hardening response.

3.1.2. Constitutive response

Zerilli and Armstrong [17,18] developed physically-based constitutive equations based on the general mechanical responses for fcc, bcc and hcp metals. The Zerilli-Armstrong equation is based on the framework of thermally-activated dislocation motion, where both the work hardening and strain-rate sensitivity are influenced by the temperature. This equation was applied by Meyers et al. [19]

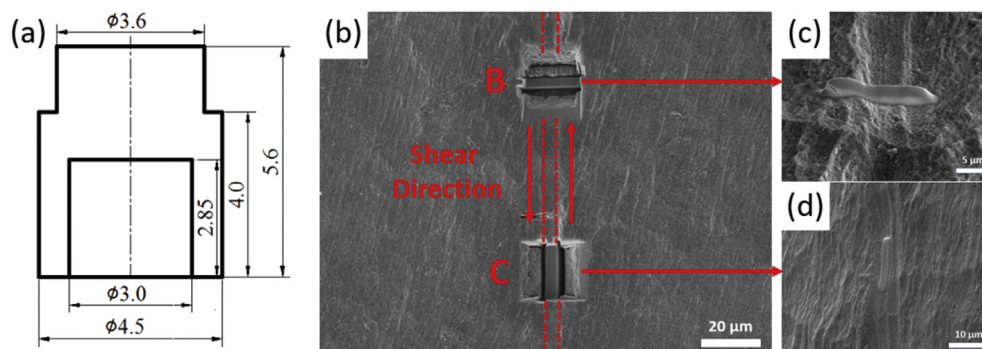


Fig. 2. (a) Schematic configuration of the hat-shaped specimen (Dimensions in mm). (b) SEM images of FIB positions. (c) Sample B position perpendicular to the shear band. (d) Sample C position along the shear band. (The edges of the shear band marked by red lines). (For interpretation of the references to colour in this figure legend, the reader is referred to the web version of this article.)

Download English Version:

<https://daneshyari.com/en/article/5436556>

Download Persian Version:

<https://daneshyari.com/article/5436556>

[Daneshyari.com](https://daneshyari.com)